

## Regulating the Translocation of DNA through Poly(*N*-isopropylacrylamide)-Decorated Switchable Nanopores by Cononsolvency Effect

Huaisong Yong,\* Bastien Molcrette, Marcel Sperling, Fabien Montel,\* and Jens-Uwe Sommer\*

Cite This: *Macromolecules* 2021, 54, 4432–4442

Read Online

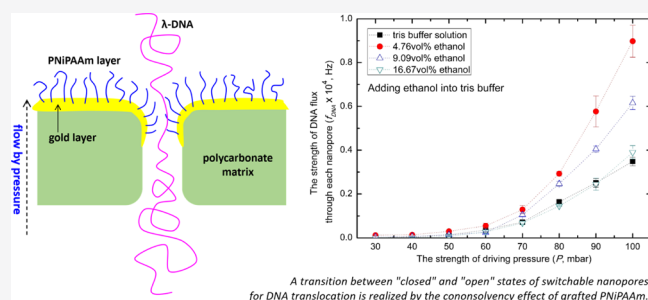
ACCESS |

Metrics & More

Article Recommendations

Supporting Information

**ABSTRACT:** Stimulus response of polymer-decorated nanopores/nanochannels is a fascinating topic both in polymer science and modern nanotechnology; however, it is still challenging for standard analytical methods to characterize these switchable nanopores/nanochannels. In this study, based on the physics of polymer translocation, we developed an analytical method and thus for the first time were able to quantitatively measure the effective thickness of the polymer layer around the rim of nanopores. As an application example of this method, we studied the translocation dynamics of fluorescence DNA through poly(*N*-isopropylacrylamide)-decorated switchable nanopores in aqueous environments. By adding small amounts of ethanol to the aqueous buffer solution, a switch-like response of the DNA translocation can be observed. It is also observed that a pronounced switching effect can be only realized in a window of moderate grafting densities of the poly(*N*-isopropylacrylamide) layer. These are attributed to the cononsolvency effect which causes a collapse of the polymer layer and thus a transition between “closed” and “open” states of the nanopores for DNA translocation. Our study clearly transpired that the cononsolvency effect of polymers can be used as a novel trigger to change the size of nanopores, in analogy to the opening and closure of the gates of cell membrane channels. We envisage that our study will spawn further developments for the design of switchable nanogates and nanopores.



### INTRODUCTION

Switch-like response in soft matter can be achieved by volume changes in immobilized polymers such as gels and polymer brushes in solution, triggered by pH, thermal, and photo-responses.<sup>1</sup> However, harnessing of these effects in applications generally requires a large change in the environmental parameters such as temperature and pH. Particularly, when considering applications in biomaterials, this is inconvenient, since in living environments, temperature and pH usually have to be controlled in a narrow range. On the other hand, it is known that volume phase transitions take place when biopolymers such as RNA are mixed with multicomponent solutes/solvents including nonspecific RNA-binding proteins.<sup>2,3</sup> Another example is re-entrance condensation of proteins in aqueous solutions observed by the addition of multivalent salts.<sup>4</sup> A phenomenon similar to re-entrance condensation of proteins is cononsolvency first observed in synthetic polymers.<sup>5,6</sup> Here, a mixture of two good solvents causes the collapse or demixing of polymers such as poly(*N*-isopropylacrylamide) (PNIPAAm) in a certain range of compositions of these two solvents. It is worth noting that this transition is of first order even for immobilized macromolecules;<sup>7</sup> thus, a small concentration change in the cosolvent is sufficient to trigger the collapse. Previous studies<sup>8</sup>

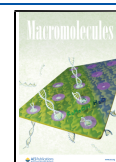
confirmed that the thickness of a PNIPAAm brush on a flat surface exhibits a switch-like response when a very small amount of alcohol (usually termed cosolvent) is added into the aqueous solutions of polymer brushes. Thus, cononsolvency of polymer brushes appears as a promising candidate to mimic the opening and closing of cell membrane channels, but so far, this is merely supported by coarse-grained computer simulations<sup>9–11</sup> and not yet reported in any experimental investigation.<sup>12–15</sup>

Meanwhile, we have to realize that it is impossible to do a rational experimental investigation on the cononsolvency response of polymer-decorated switchable nanopores, unless suitable characterizing methods are available. However, it remains very challenging for standard analytical methods to characterize stimulus-responsive behaviors of polymer layers in various confined environments such as nanopores. To the best of our knowledge, only few studies<sup>16–18</sup> reported that atomic

Received: January 28, 2021

Revised: April 11, 2021

Published: April 23, 2021



force microscopy can be used to qualitatively detect the hydrodynamic thickness of a polymer layer around the hollow structures. The lack of analytical methods to quantify the thickness of a polymer layer around the rim of nanopores actually impedes further developments for the rational design of functionalized nanogates and nanopores<sup>12–15,19–21</sup> for applications such as the sensing of single molecules.<sup>22–27</sup>

Hence, it is an important aim of this work to develop a method to quantitatively determine the thickness of a polymer layer around the rim of nanopores. In this study, we achieved this task on the basis of the physics of polymer translocation. As an application example of this method, we studied the translocation dynamics of fluorescence DNA through PNiPAAM-decorated switchable nanopores in aqueous environments. We demonstrated that switchable nanopores can be prepared by harnessing the cononsolvency transition in grafted polymers. The widening of the PNiPAAM-decorated nanochannels occurs in a narrow window of about 5% volume fraction of ethanol in aqueous buffer solution. Experimental results quantitatively showed that PNiPAAM layers around the rim of nanopores show solvent-composition-responsive behaviors in the range of metabolic pH values and room temperatures. In the following, the methodology used in this study will be first described in the section **Experiments and Methods**, then experimental results will be discussed in the section **Results and Discussion**, and finally, concluding remarks will be made in the section **Conclusions**.

## EXPERIMENTS AND METHODS

**DNA Translocation Experiments.** In our experiments, track-etched polycarbonate membranes (Whatman, with nominal pore diameters equal to 50 nm and thicknesses equal to 6  $\mu\text{m}$ ) were used in DNA translocation experiments. First, the membranes are one-side-sputtered with a thin layer of gold (EVA 300 Alliance Concept evaporator, thickness 50 nm, speed of deposit 0.2 nm). A typical scanning electron microscopy image of the gold-coated nanopores used in DNA translocation experiments in this study is shown in **Figure 1**. The polydispersity of the sizes of the nanopores is rather

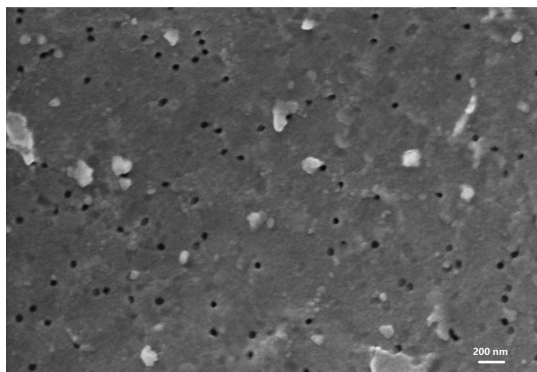


**Figure 1.** Typical scanning electron microscopy image of the gold-coated nanopores used in DNA translocation experiments in this study. The dark circles in the image are nanopores.

low, the boundary for the diameter is about  $50 \pm 10$  nm, and similar nanopores were already used in our previous investigations.<sup>28</sup> Then, the gold layer is grafted with a PNiPAAM layer by the grafting-to synthetic method. In this study, the different samples are named “higher-graft-15K” and “lower-graft-15K” to discriminate the higher and lower grafting densities of polymer layers with a molecular weight of  $M_n = 1.5 \times 10^4$  g/mol and a dispersity of  $M_w/M_n = 1.18$ . We named “higher-graft-30K” and “lower-graft-30K” to discriminate the

higher and lower grafting densities of polymer layers with a molecular weight of  $M_n = 3.0 \times 10^4$  g/mol and a dispersity of  $M_w/M_n = 1.25$ . For the details of preparation of these polymer layers, see Section S1.1 of the **Supporting Information**.

As for DNA translocation experiments, a dilute solution of  $\lambda$ -DNA (0.1 pM, 48 kbp) in tris buffer solution (tris 10 mM, EDTA 1 mM, and KCl 10 mM, pH  $\approx$  7.6) fluorescently labeled with YoYo-1 (Life Tech) was filled in the cis-chamber where the pressure was applied, for the experimental details, please refer to our previous publications such as ref 28. A few hundred DNA translocation events were observed simultaneously with a time resolution of about 10 ms by fluorescence microscopy, which was sufficient to resolve each translocation event. A cartoon depiction of  $\lambda$ -DNAs translocating through PNiPAAM-grafted nanopores is shown in **Figure 2**.

In our cononsolvency experiments, ethanol is merely added to the buffer solution in the trans-chamber, see **Figure 2b**. It is worth noting that the volume size of the trans-chamber is significantly larger than that of the cis-chamber; thus, in our study, the solvent-composition change in the trans-chamber due to buffer solutions (without ethanol) driven from the cis-chamber can be neglected.

Because the trans-side of the membrane including a part of the nanochannel is coated with a gold layer, the direct contact between the solvent and polycarbonate matrix in the trans-side is actually blocked and the infiltration of ethanol on the polycarbonate matrix unlikely happens when taking into account that the pressure on the cis-side of the membrane causes a flow from the cis- to the trans-chambers. Thus, it is unlikely that the DNA translocation in the nanochannel is directly affected by the addition of ethanol in the trans-chamber. This was confirmed by our control experiments for a blank membrane (without grafting PNiPAAM layers) in various mixtures of ethanol and tris buffer, for details, see Section S2 of the **Supporting Information**. In addition, the analytical method to determine the thickness of nanopore brushes that we developed in this work (see the section of **Method of Characterizing Nanopore-Brush Thickness**) relies on the system at a steady state under the flow pressure from the cis- to the trans-chambers. Before collecting data, it is necessary to wait for a period of time to make sure that the system is at steady state when the driving pressure is changed in experiments. In our experiments, this waiting time is about 2 min. This approach can also help to effectively eliminate the possible influence of ethanol infiltration on the polycarbonate nanochannel in our cononsolvency experiments.

Although ethanol addition obviously affects the DNA conformation in the trans-chamber (after translocation) when the volume fraction of ethanol is high (the threshold value is about 40% in our study when the solvent becomes poor for DNA), we note that the most interesting effects occur for very low ethanol concentrations far below the threshold value of 40%. The poorer solvent quality in the trans-chamber implies a chemical potential or solubility gradient acting against the translocation. Since we see a clear re-entrance behavior at higher alcohol concentrations, this effect is apparently only of minor importance for the observation of the gating behavior of the pores.

**Method of Characterizing Nanopore-Brush Thickness.** In this study, to quantitatively estimate the thickness of the polymer layer around the rim of nanopores, we used the celebrated suction model for the translocation of polymer in dilute solutions introduced by de Gennes.<sup>29,30</sup> Our method is on the basis of the DNA translocation efficiency which in turn relies on the proven fact that in the strong confinement regime, the critical force to guide flexible linear polymer chains through nanopores is independent of the chain length.<sup>31</sup> We analyzed the variation of the DNA translocation frequency per pore ( $f_{\text{DNA}}$ ) with the driving force such as the gradient of flow pressure, see **Figure 2b**. In the framework of the suction model,<sup>28,32</sup> the translocation frequency is expressed as

$$f_{\text{DNA}} = k_1 \exp\left(-\frac{\Delta F}{k_B T}\right) \quad (1)$$

by assuming that DNA translocation is described as the travel of a flexible polymer through a free-energy landscape with a barrier of

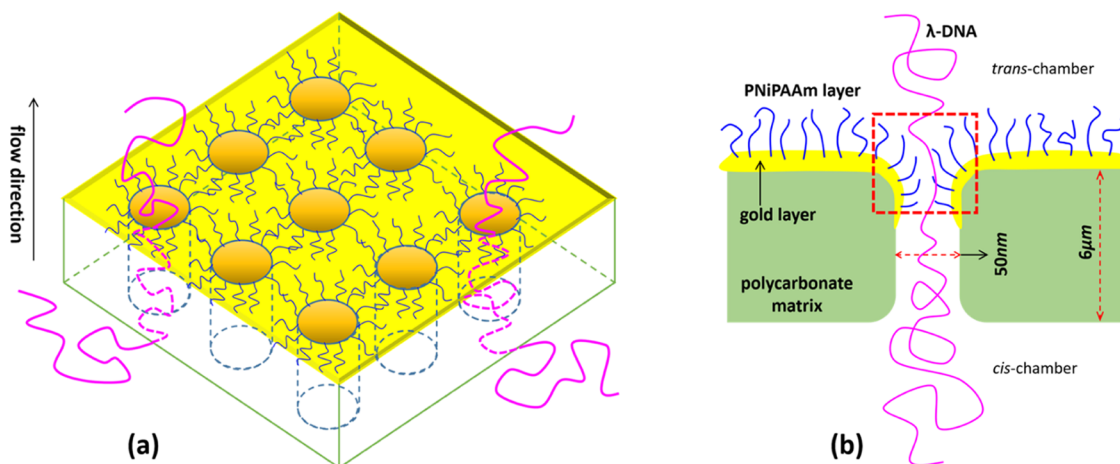


**Figure 2.** Sketch of fluorescence  $\lambda$ -DNAs translocating through PNiPAAm-grafted nanopores: (a) three-dimensional view of nanopore structures and (b) side view of a single nanopore. In this study, based on the DNA translocation efficiency, we developed an analytical method to quantitatively measure the effective thickness of a polymer layer around the rim of nanopores, that is, the polymer layer in the box region depicted in (b).

height  $\Delta F$  and assuming that the translocation process follows a Boltzmann statistic. We note that the persistence length of DNA is about 50 nm which is also the nanopore size in this study; thus, a flexible polymer-chain assumption for DNA in this study is reasonable.<sup>33</sup>

In eq 1,  $k_B$  is the Boltzmann constant and  $T$  is the thermodynamical temperature.  $k_1$  (Hz) is the rate of incidence on the barrier. By Kramers' theory<sup>34,35</sup> for Brownian motion in a field of force, when  $k_1$  is dominated by the presence of the barrier  $\Delta F$ ,  $k_1 \propto J/J_c$  holds with  $J$  being the solvent flux ( $\text{m}^3 \text{s}^{-1}$ ) and  $J_c$  being the solvent-flux threshold. In the suction model, the energy barrier is  $\Delta F = k_B T (J_c/J)$  and the translocation frequency  $f_{\text{DNA}}$  finally reads

$$f_{\text{DNA}} = k_2 \left( \frac{P}{P_c} \right) \exp \left( - \frac{P_c}{P} \right) \quad (2)$$

with  $k_2$  being a proportionality factor (Hz),  $P$  being the gradient of pressure applied by the equipment where the pressure on the side of the membrane without coating a gold layer is higher, and the critical pressure  $P_c = r_h J_c$ . The hydrodynamical resistance of the pore  $r_h$  equals to  $8\eta L / \pi R_{\text{eff}}^4$  with  $L$  being the length of a pore ( $L = 6 \mu\text{m}$  in this study) by Poiseuille's law,  $R_{\text{eff}}$  being the effective radius of pores, and  $\eta$  being the solvent viscosity in the cis-chamber, see Figure 2b. In this study,  $\eta$  is the solvent viscosity of the tris buffer (without ethanol).

Taking into account of the fact that the pore size is significantly larger than the cross-sectional size of DNA backbone and the Reynolds number is at the order of about  $10^{-4}$ , the Poiseuille's law and Darcy's law are still valid for the flow in this study.<sup>28,36</sup> Keeping in mind that the solvent-flux threshold ( $J_c$ ) of polymer translocation has been proven by both theories<sup>29,30</sup> and experiments<sup>31</sup> at the order of

$$J_c = \text{const} \times \frac{k_B T}{\eta} \quad (3)$$

then we can use this relation to estimate the thickness of a polymer layer around the rim of nanopores. Technically speaking, it is unnecessary to know the numerical prefactor on the right-hand side of eq 3 in experiments; the effective (hydrodynamic) radius of the polymer-decorated pore,  $R_{\text{eff}}$ , can be calculated in a way of avoiding the numerical prefactor as mentioned below

$$R_{\text{eff}} = R_0 \left( \frac{P_{c,0}}{P_{c,\text{eff}}} \times \frac{T_{\text{eff}}}{T_0} \right)^{1/4} \quad (4)$$

where  $P_{c,0}$  and  $P_{c,\text{eff}}$  are critical pressures of the blank membrane and when the same membrane is grafted with a polymer layer, respectively, and  $T_0$  and  $T_{\text{eff}}$  are temperatures where experiments

are conducted for the blank membrane and when the same membrane is grafted with a polymer layer, respectively. In our consolvency experiments, the temperature is fixed at 298 K; thus,  $T_{\text{eff}} = T_0$  holds in our experiments.  $R_0$  is the radius of nanopores without grafted polymers, usually it is insensitive to normal temperature change; in this study,  $R_0 = 25.0 \pm 1.0 \text{ nm}$  is the corresponding measured mean value with an average absolute deviation using scanning electron microscopy (Figure 1).

Taking into account the fact that the polymer layer was grafted around the rim of nanopores, the relation of  $R_{\text{eff}} \leq R_0$  always holds. Then, the effective thickness of the polymer layer around the rim of nanopores can be obtained as

$$H = R_0 - R_{\text{eff}} \quad (5)$$

that is, the effective thickness of the polymer layer in the box region is depicted in Figure 2b. It is remarkable that eq 4 is a fourth-order power law, and this implies that the change of critical pressure is sensitive to the change of pore size and thus the effective thickness of the polymer layer around the rim of nanopores can be estimated in a relatively high accuracy. It is noted that we measure  $H$  under flow conditions which leads to the fact that the estimated thickness ( $H$ ) may not coincide with the thickness of equilibrium polymer layers.

DNA translocation frequency per pore  $f_{\text{DNA}}$  is calculated as

$$f_{\text{DNA}} = \frac{N_{\text{DNA}}}{\rho_{\text{pore}} A t} \quad (6)$$

The DNA translocation efficiency, that is, the number of DNA translocation events ( $N_{\text{DNA}}$ ) through a fixed area ( $A = 135 \mu\text{m} \times 135 \mu\text{m}$ ) of membranes and in a fixed period of time ( $t = 30 \text{ s}$ ) observed in the trans-chamber is counted by a combination of both visual inspection by human eyes and using an in-house script coded in Python. Examples to determine the number of DNA translocation events are shown in Figure S1 of the Supporting Information and Video Supporting Information. For the details of how to count the number of DNA translocation events and process these data, see Sections S1.2–1.4 of the Supporting Information.

The pore density in eq 6 is with a value of  $\rho_{\text{pore}} = 6 \times 10^8 \text{ pores/cm}^2$  in this study. The average number of pores in the fixed area is about  $1.1 \times 10^5$ ; thus, the observed number fluctuation of DNA translocation events in this study actually can be neglected. As shown in eq 6, the number of translocation events ( $N_{\text{DNA}}$ ) observed in this study only differs from the translocation frequency ( $f_{\text{DNA}}$ ) by a constant multiplicative factor. In this study, the critical pressure ( $P_c$ ) is obtained by fitting the nonlinear equation eq 2, the detail of using eq 2 to process experimental data in this study is shown in Section S1.4 of the Supporting Information.

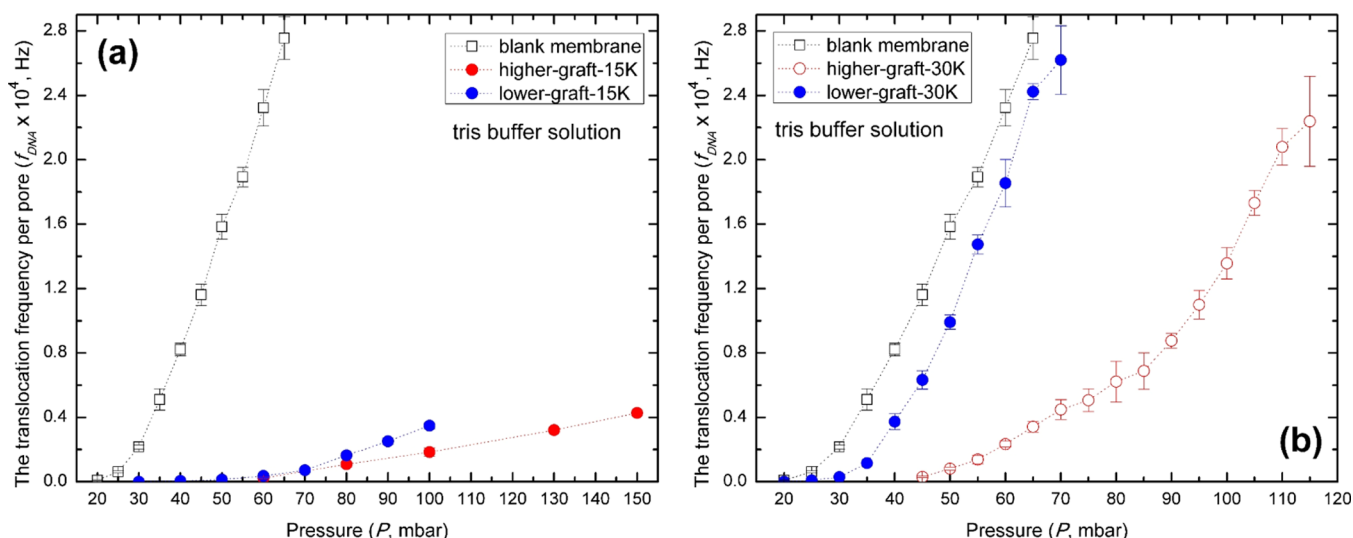


**Figure 3.** Translocation frequency of DNA per pore with respect to pressure. (a) Grafting-density effect of different PNiPAAm layers with a shorter polymer chain in tris buffer, the molecular weight of PNiPAAm layers is  $M_n = 1.5 \times 10^4$  g/mol, and dispersity is  $M_w/M_n = 1.18$ . (b) Grafting-density effect of different PNiPAAm layers with a longer polymer chain in tris buffer, the molecular weight of PNiPAAm layers is  $M_n = 3.0 \times 10^4$  g/mol, and dispersity is  $M_w/M_n = 1.25$ . The pH value of the buffer is about 7.6, and measurement temperature is 25 °C. The dotted lines in the figures are guides to eyes.

We note that the driving force for DNA translocation through nanopores/nanochannels can be an electric field<sup>19,37</sup> which is widely used in translocation experiments and still lack quantitative methods to characterize, and our experimental method can be extended and formulated to this case. Following a rationale in analogy to the case of pressure driving as shown above, for the case of electric field as the driving force, the translocation frequency  $f_{DNA}$  reads as<sup>38</sup>

$$f_{DNA} = k_3 \left( \frac{E}{E_c} \right) \exp\left( -\frac{E_c}{E} \right) \quad (7)$$

with  $k_3$  being a proportionality factor (Hz),  $E$  being the strength of the electric field applied to drive DNA translocation, and  $E_c$  being the electric field threshold. In experiments, the voltage strength  $V = EL$  is usually used instead of the electric field strength ( $E$ ) with  $L$  being the length of a pore (such as  $L = 6 \mu\text{m}$  in this study).

It is remarkable that from experimental observations,<sup>28,38–40</sup> DNA translocation behavior can be qualitatively separated by the free-energy barrier of translocation into two distinct regimes. When the driving force is lower or comparable to the free-energy barrier, diffusive and slow dynamics can be approximated by an exponential increase with the external force. When the driving force is significantly larger than the free-energy barrier, it asymptotically approaches a linear increase. This heterogeneous behavior is also verified by the hydrodynamic derivation of eqs 2 and 7. The applicability of eq 7 can be verified by experimental data reported by refs.<sup>38–40</sup> It is worth noting that one can estimate the free-energy barrier for a successful polymer translocation using eqs 2 and 7; it is at the order of several  $k_B T$  and agrees with the prediction of the scaling theory as already reported in our previous work.<sup>28</sup>

For the case of electric field as the driving force, the electric field threshold ( $E_c$ ) to overcome the free-energy barrier of polymer translocation is bias-equivalent to the critical flux in the suction model and is scaled at the order of

$$E_c = \text{const} \times \frac{k_B T}{qR^3} \quad (8)$$

with  $R$  being the pore radius.<sup>38</sup> Taking into account that for controlled experiments, the surface charge density ( $q$ ) of polymer “blobs” in the nanopore usually is a constant and insensitive to normal temperature change; the effective (hydrodynamic) radius of the

polymer-decorated pore,  $R_{eff}$ , can be calculated in a similar way like eq 4

$$R_{eff} = R_0 \left( \frac{E_{c,0}}{E_{c,eff}} \times \frac{T_{eff}}{T_0} \right)^{1/3} \quad (9)$$

where  $E_{c,0}$  and  $E_{c,eff}$  are electric field thresholds of the blank membrane and when the same membrane is grafted with a polymer layer, respectively. Note that the exponent difference between eqs 4 and 9 implies that a pressure-controlling experiment is preferable; compared with the change of electric field threshold, the change of critical pressure is much sensitive to the change of pore size. Nevertheless, one advantage of translocation experiments by electric field driving is that the translocation frequency ( $f_{DNA}$ ) can be easily and accurately obtained via the analysis of electric current signals with respect to time trace.

Let us mention that our experimental method is an ensemble-average approach and the statistical quality of the results depends on a sufficiently high pore density in the membrane. The basic assumption of our method is that the DNAs have a radius of gyration larger than the pore diameter and they are in the dilute regime of the DNA solution. We also note that in the translocation experiments, other polymers can also be used such as proteins<sup>23–25</sup> and synthetic polymers,<sup>41,42</sup> in principle, our experimental methods can be extended without difficulty to these cases; however, this topic is beyond the scope of this study.

## RESULTS AND DISCUSSION

**Results of DNA Flux through (PNiPAAm-Decorated) Nanopores.** Our experimental results of the translocation frequency of DNA per pore in a tris buffer solution as a function of pressure are displayed in Figure 3. We compare the results for blank membranes (with a gold layer) and for different grafting densities of PNiPAAm. For different grafting densities, the translocation efficiency, that is, the translocation frequency of DNA per pore at a given pressure, is reduced dramatically as compared to the bare or blank membrane. At higher pressure, the higher grafting density leads to a higher reduction of the translocation efficiency in accordance with the fact that higher grafting densities lead to thicker polymer layers when the chain lengths of grafted polymers are the same. With

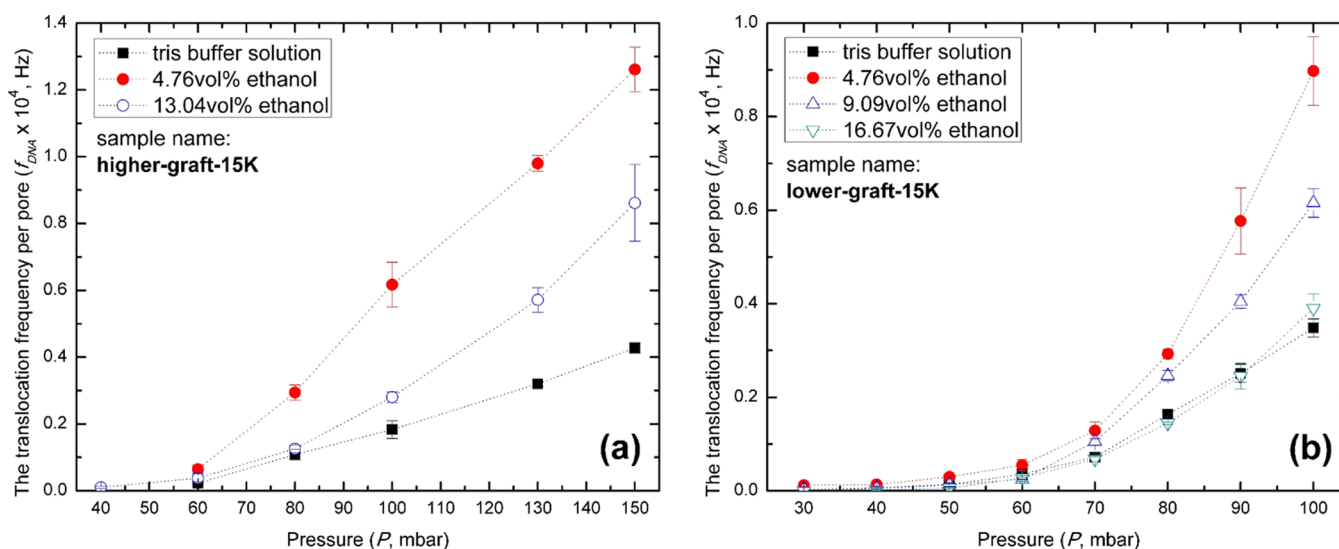


**Figure 4.** Translocation frequency of DNA per pore with respect to pressure. Solvent-composition response of different PNiPAAm layers: (a) for a membrane of a higher grafting density and (b) for a membrane of a lower grafting density. The molecular weight of PNiPAAm layers is  $M_n = 1.5 \times 10^4$  g/mol, and dispersity is  $M_w/M_n = 1.18$ . The pH value of the buffer is about 7.6, and measurement temperature is 25 °C. The dotted lines in the figures are guides to eyes.

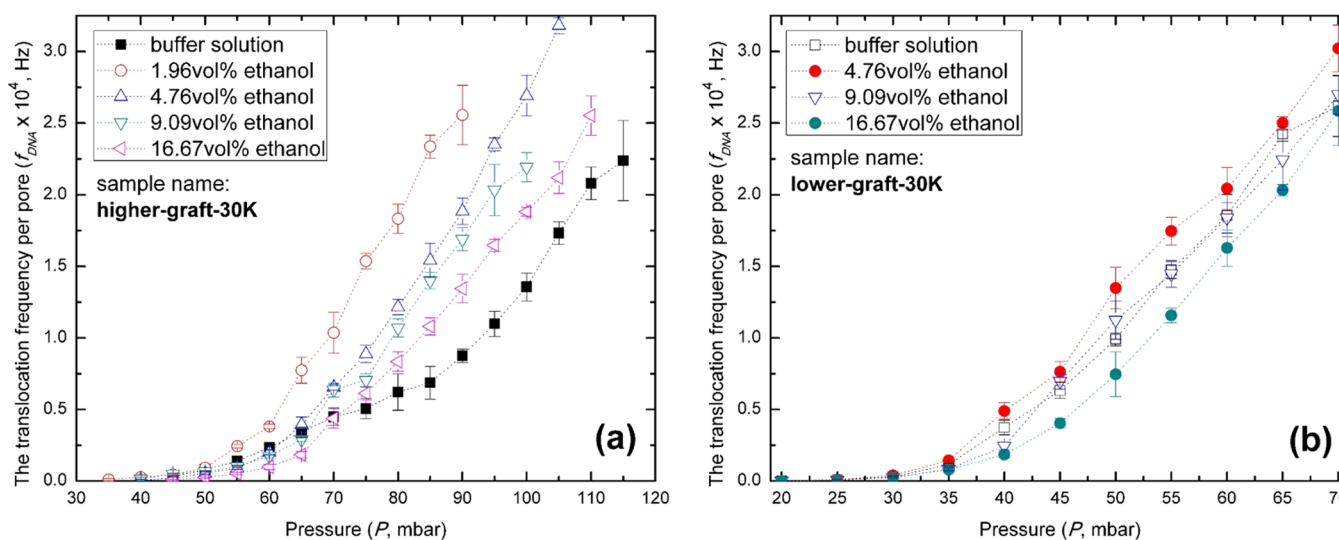


**Figure 5.** Translocation frequency of DNA per pore with respect to pressure. Solvent-composition response of different PNiPAAm layers: (a) for a membrane of a higher grafting density and (b) for a membrane of a lower grafting density. The molecular weight of PNiPAAm layers is  $M_n = 3.0 \times 10^4$  g/mol, and dispersity is  $M_w/M_n = 1.25$ . The pH value of the buffer is about 7.6, and measurement temperature is 25 °C. The dotted lines in the figures are guides to eyes.

the help of a scaling analysis, we can show that the polymer layers displayed in Figure 3a are in a brush state, while the polymer layers displayed in Figure 3b are below the brush state; for details, see Section S1.5 of the Supporting Information.

As shown in Figures 4 and 5, for each membrane with a PNiPAAm layer, the translocation frequency of DNA per pore first increases with an increase of ethanol concentration. With further increase of ethanol concentration, the translocation frequency of DNA per pore decreases again. This implies that the size of the nanopores first increases under the stimuli of increasing ethanol concentration, later the nanopore size reduces by further increasing ethanol concentration. This indicates that grafted PNiPAAm shows re-entrance signature of cononsolvency transition in the ethanol/tris buffer mixtures, as observed for flat brushes.<sup>8</sup> This observation is clearly

supported by a study of the normalized translocation frequency of DNA per pore which is plotted with respect to the change of ethanol concentration under different driving pressures, see Figures 6 and S5 (Supporting Information). Solvent-composition-responsive behaviors shown in Figures 4–6 and S5 indicate that the cononsolvency effect of grafted PNiPAAm can be used to control the size of nanopores.

In Figures 4b and 5a, it is noted that for polymer layers with moderate-grafting densities, when the applied flow pressure is low and in a certain range, DNA can translocate through PNiPAAm-decorated nanopores at very low concentrations of ethanol (4.76 and 1.96% vol, respectively) but not at much higher concentrations of ethanol and in tris buffer. This phenomenon is unavoidably attributed to the cononsolvency effect which causes a collapse of the polymer layer and thus a transition between “closed” and “open” states of the nanopores

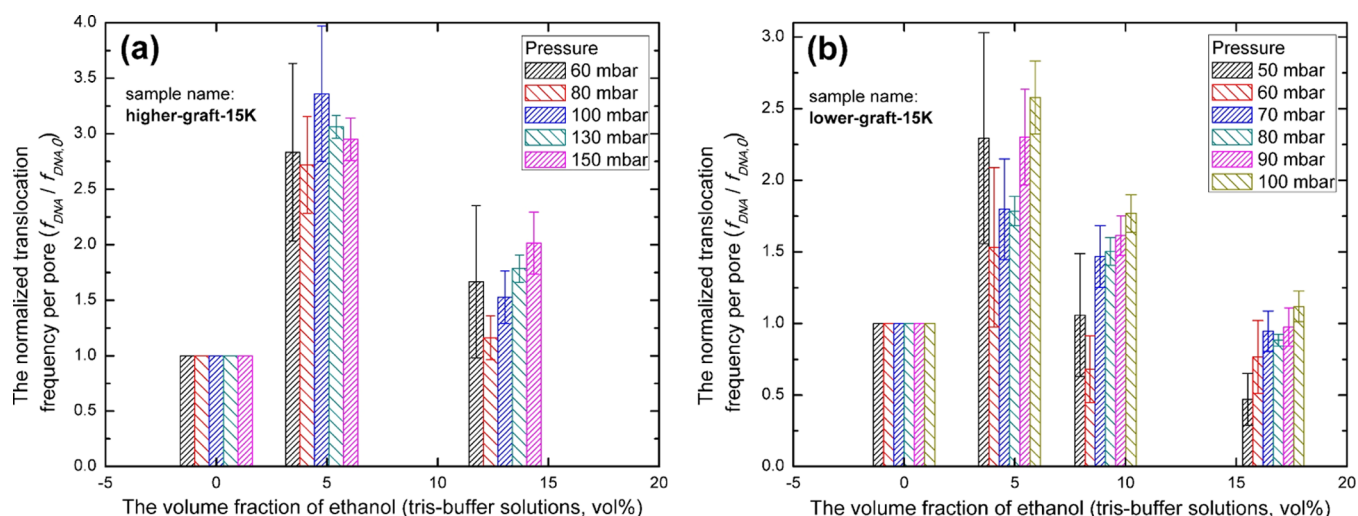


**Figure 6.** Normalized translocation frequency of DNA per pore is plotted with respect to ethanol concentration change under different driving pressures. (a) For a higher grafting density of PNiPAAm-grafted nanopores, data are the same as in Figure 4a. (b) For a lower grafting density of PNiPAAm-grafted nanopores, data are the same as in Figure 4b. Note that  $f_{DNA,0}$  is the observed translocation frequency of DNA per pore in tris buffer solutions (no addition of ethanol). From the left-hand to the right-hand sides of the figure, column bars arrange the pressure in increasing order.

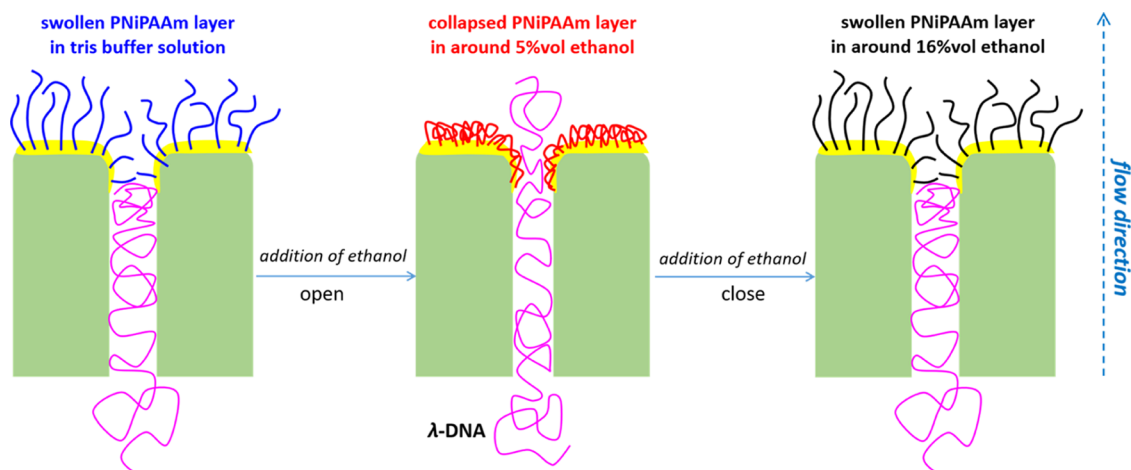


**Figure 7.** For a polymer layer with a moderate-grafting density, when the applied flow pressure is low and in a certain range, the DNA translocation through PNiPAAm-decorated nanopores can be regulated by the addition of ethanol to tris buffer solutions. This phenomenon is attributed to the consolvency effect which causes a collapse of the polymer layer and thus a transition between “closed” and “open” states of the nanopores.

for DNA translocation. Under the condition of flow pressure, a depiction of DNA translocation and ethanol concentration-induced phase transition of a PNiPAAm layer around the rim of nanopores is shown in Figure 7.

In Figure 8, we display the results for both grafting densities at the opening of PNiPAAm-grafted nanopores at 4.76% vol of ethanol. Comparing results for both grafting densities in tris buffer (Figure 3) and 4.76% vol of ethanol (Figure 8), we observe a consistent increase of DNA translocation efficiency with decreasing grafting density of the polymer layer. We made control experiments for nanopores which had no grafted PNiPAAm and verified that the direct effect of ethanol on the translocation behavior of DNA was actually negligible, see Figure S6 (Supporting Information); also, ethanol has no swelling effect on the matrix material (gold-coated polycarbonate) used to manufacture nanopores in this study. It should be particularly pointed out that the observed re-entrance behaviors of DNA translocation in Figures 4 and 5 can hardly be ascribed to the possible infiltration of ethanol on the

polycarbonate nanochannels because the ethanol infiltration can merely lead to a monotonous change with an increase of ethanol concentration and therefore the re-entrance behaviors of DNA translocation shall not be observed at all on account of ethanol infiltration. Therefore, the origin of the non-monotonous opening/closing behavior of the nanochannel can be merely the solvent response of the grafted PNiPAAm. These results are in agreement with our previous studies of flat brushes, where a nonmonotonous change of the brush height reaches a minimum at low alcohol concentrations.<sup>8</sup>

Let us add some remarks about the effect of polydispersity of bare pore size on our results. The polydispersity of the bare membrane in our study is rather low (with a boundary of diameter about  $50 \pm 10$  nm, see Figure 1) and thus smaller or larger pores should not lead to a qualitatively different translocation behavior. Nevertheless, a priori averaging over all translocation events through the membrane reduces the contrast between “open” and “closed” pores in the consolvency response. Thus, our ensemble-averaged meas-

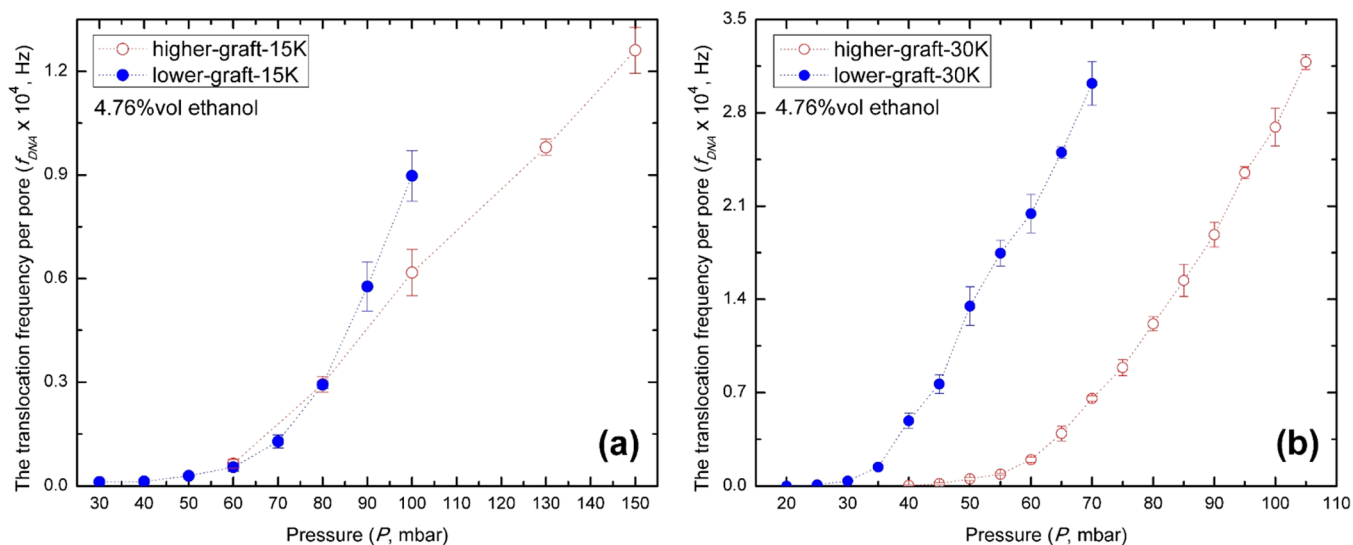


**Figure 8.** Translocation frequency of DNA per pore with respect to pressure. Grafting-density effect of different PNiPAAm layers in 4.76% vol ethanol/tris buffer mixtures when DNAs translocate through nanopores. (a) Membranes with the molecular weight of PNiPAAm layers  $M_n = 1.5 \times 10^4$  g/mol, and dispersity is  $M_w/M_n = 1.18$ . (b) Membranes with the molecular weight of PNiPAAm layers  $M_n = 3.0 \times 10^4$  g/mol, and dispersity is  $M_w/M_n = 1.25$ . The pH value of the buffer is about 7.6, and measurement temperature is 25 °C. The dotted lines in the figures are guides to eyes.

**Table 1. Reference Values for the Swollen Thickness of PNiPAAm Layers Around the Rims of Nanopores in Mixtures of Tris Buffer Added with Various Concentrations of Ethanol<sup>a</sup>**

sample name	grafting density (chains/nm <sup>2</sup> )	tris buffer (nm)	1.96% vol (nm)	4.76% vol (nm)	9.09%vol (nm)	13.04%vol (nm)	16.67%vol (nm)	Morphology
higher-graft-15K	~0.30	10.0 ± 1.0		8.5 ± 0.1		9.0 ± 0.5		brush
lower-graft-15K	~0.15	7.0 ± 0.1		3.8 ± 0.1	6.3 ± 0.1		7.5 ± 0.5	brush
higher-graft-30K	~0.05	5.3 ± 0.1	3.5 ± 0.1	4.3 ± 0.1	4.2 ± 0.1		4.5 ± 0.1	mushroom/brush <sup>b</sup>
lower-graft-30K	≪0.05	1.6 ± 0.1		1.2 ± 0.1	1.4 ± 0.1		2.1 ± 0.1	mushroom

<sup>a</sup>The layer thickness and its error bars are calculated based on the data of the translocation frequency of DNA per pore reported in Figures 3–5. These data are calculated by the analytical method developed in this study, for details, see the section **Method of Characterizing Nanopore-Brush Thickness**. <sup>b</sup>It is hard to determine the exact morphology for this sample merely based on a scaling analysis.

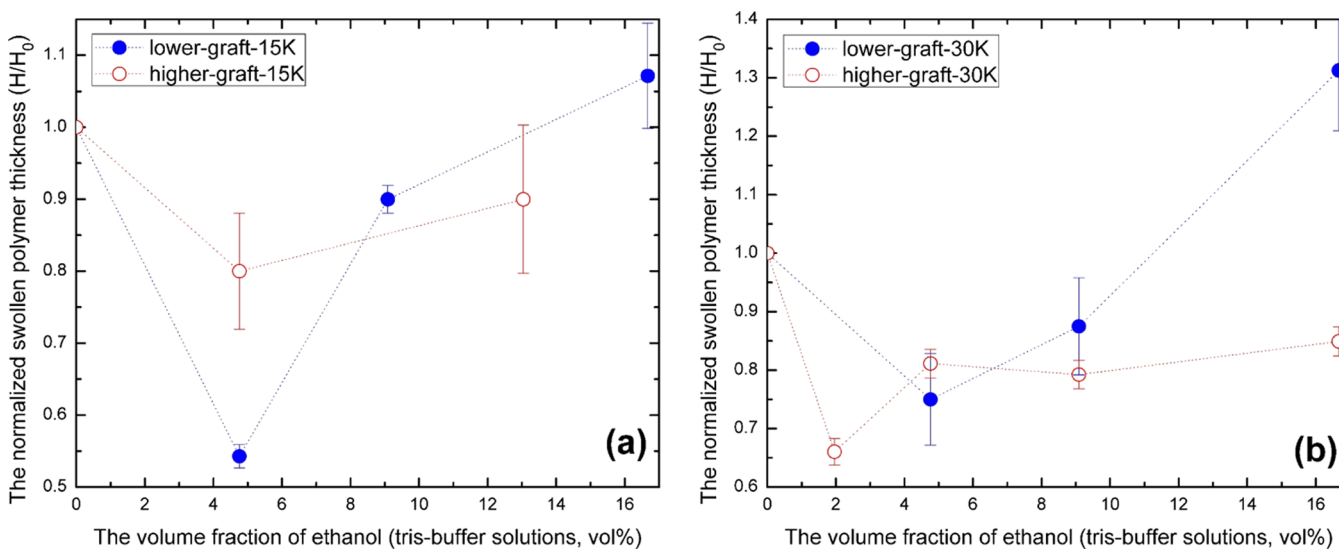


**Figure 9.** Ethanol-concentration response of grafted PNiPAAm polymers around the rim of nanopores, and the relative polymer thickness is calculated by the data reported in Table 1. (a) Membranes with the molecular weight of PNiPAAm layers  $M_n = 1.5 \times 10^4$  g/mol and dispersity  $M_w/M_n = 1.18$ . (b) Membranes with the molecular weight of PNiPAAm layers  $M_n = 3.0 \times 10^4$  g/mol and dispersity  $M_w/M_n = 1.25$ . The pH value of the buffer is about 7.6, and measurement temperature is 25 °C. The dotted lines in the figures are guides to eyes.

urements give a lower boundary for the quality of the switching response which could be achieved under ideal monodisperse condition. An interesting and may be somewhat counter-

intuitive conclusion can be drawn from the interplay between the grafting-to synthetic method and the variation of bare pore size: Since larger pores lead to less geometric constraints for

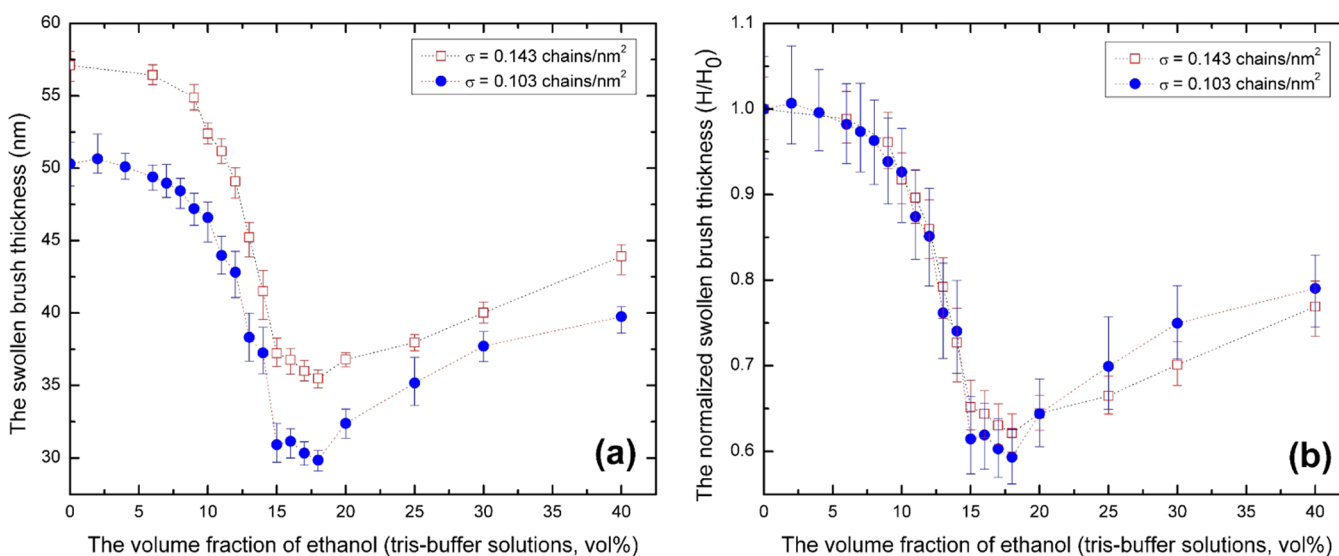


**Figure 10.** Study of in situ vis-spectroscopic ellipsometry for equilibrium swollen brush thickness on grafting-density effect in the cononsolvency transition of PNiPAAm brushes in ethanol/tris buffer mixtures on the flat surface, at the temperature of 25 °C and the pH value of the buffer is 7.45: (a) absolute swollen brush thickness and (b) normalized swollen brush thickness. Experiments were conducted with the molecular weight of  $M_n = 6.1 \times 10^4$  g/mol and  $M_w/M_n = 1.40$  for all polymer brushes. The dotted lines in the figures are guides to eyes.

the polymer grafting reaction, a higher grafting density and thus a larger height of the resulting polymer layer can be expected. This reduces the effective size variation of the polymer-coated pores.

**Comparative Study between Nanopore Brushes and Flat Brushes.** While our experimental results of DNA flux through nanopores are in agreement with our present understanding of the cononsolvency effect in grafted polymer layers for flat surfaces, the abovementioned discussions are still qualitative so far. To get some quantitative insights, we used the experimental results in Figures 3–5 to calculate the reference values for the absolute height of PNiPAAm layers around the rim of nanopores using eqs 2, 4, and 5, and the results are displayed in Table 1. The grafting densities and morphological regimes of polymer layers in this study were also estimated, see Table 1; for details, see Section S1.5 of the Supporting Information.

In Figure 9, we also display the normalized swollen thickness of polymer layers which are grafted around the rim of nanopores. It is observed that in Figure 9a, an increase of grafting density of nanopore brushes weakens the collapse transition of the brush layer in ethanol/tris buffer mixtures, this follows the analytic prediction of a mean-field model for cononsolvency transition by our previous studies.<sup>7,43</sup> Also, as shown in Figures 5b and 9b, a PNiPAAm polymer layer with very low grafting density below the brush state still displays re-entrance behavior; however, the corresponding phase-transition behaviors are not pronounced. It becomes clear that a pronounced switching effect can only be realized in a window of moderate grafting densities.

From Figure 9b, we observed that a decrease in grafting density weakens the collapse regarding the normalized swollen polymer thickness, in contrast to the behavior shown in Figure 9a. The reason behind this observation is that the grafting-to synthetic approach leads to much lower grafting densities for the high-molecular-weight polymers, see the second column of Table 1. This in turn leads to particular morphologies in the collapsed state such as octopus-shape micelles or collapsed globules,<sup>44–47</sup> see the last column of Table 1. In turn, the

hydrodynamic thickness variation of such sparsely grafted polymer layers displays only weak variation as compared with the dense brush regime. Nevertheless, it is interesting to observe that regardless of whether the polymer layer is in a brush state, the grafting density has only a very small effect on the solvent-composition location of the maximum collapsed state. All these abovementioned cononsolvency behaviors are also observed for grafted PNiPAAm polymers on the flat surface both in ethanol/water mixtures<sup>8</sup> and in ethanol/tris buffer mixtures, see Figures S7 and S8 (Supporting Information).

Figure 10 shows measurements of in situ vis-spectroscopic ellipsometry for equilibrium swollen thickness of two PNiPAAm brushes with different grafting densities on the flat surface which are immersed in tris buffer/ethanol mixtures, for more results, also see Figures S8–S10 (Supporting Information). The methods of preparing these flat brushes and conducting ellipsometry experiments were reported in our previous studies.<sup>48</sup> The ellipsometry study clearly indicates that PNiPAAm brushes undergo a collapse with respect to an increase of ethanol concentration; also, at higher concentration of ethanol, the PNiPAAm brushes show re-entrance behavior. It also indicates that an increase of grafting density of PNiPAAm flat brushes weakens the collapse transition of flat brushes in ethanol/tris buffer mixtures provided that the collapsed brush displays a homogeneous morphology. In addition, it is of interest to see that from the right branch of the re-entrance transition for the relative brush thickness (Figures 9a and 10b), both nanopore brushes and flat brushes show similar re-entrance behaviors regarding the change of grafting density. These ellipsometry observations qualitatively cross-verified our DNA translocation experiments.

From the comparison of Figures 9 and 10, it should however be noted that the phase-transition window detected by translocation experiments through nanopores under non-equilibrium conditions differs from the window detected by ellipsometry experiments at equilibrium states. The reason for this discrepancy may be attributed to the fact that the brush is subjected to flow fields, osmotic pressure induced by the

translocating DNA, and hydrostatic pressure effects. From the theoretical description of the cononsolvency transition in brushes and in solutions,<sup>7,49</sup> it is known that densification of the polymer due to external forces shifts the cononsolvency transition to smaller cosolvent (ethanol) concentrations. It is worthy of addressing that from the comparison of Figures 9a and 10b, it can be seen that despite the shift in the transition window, the reduction of relative height in the flat brush corresponds to the change of the radius of the polymer-grafted nanopore when the grafting density is at the same level, see the data of blue circles in Figure 9a and data in Figure 10b, this can be analytically predicted by our previous theoretical studies for brush layers;<sup>7,43</sup> readers who are interested in theoretical details, please refer to our previous publications.<sup>7,43</sup>

## CONCLUSIONS

In summary, one contribution of our study is that we demonstrated that small amounts of ethanol admixed to an aqueous solution can regulate the translocation of DNA through polymer-decorated nanopores. We can identify the cononsolvency effect as being responsible for this observation which causes an abrupt collapse of the brush by increasing the alcohol content of the aqueous solution followed by reswelling at higher alcohol concentration. Regardless of the grafting density of a grafted PNiPAAM polymer layer around the rim of nanopores, in the alcohol–tris buffer mixtures, the polymer layer displays solvent-composition-responsive behaviors in the range of metabolic pH values and room temperatures. Our study also shows that a pronounced switching effect can be only realized in a window of moderate grafting densities of PNiPAAM layers. Although in this study, PNiPAAM was chosen as a model synthetic polymer, due to the universality of the cononsolvency effect in competitive solvents, the conclusions made for PNiPAAM can be extended to other synthetic polymers as well as to biopolymers.<sup>4,50</sup> As a proof of concept of using synthetic polymers to mimic biological functions of cell membrane channels,<sup>9,51</sup> our study clearly transpired that the cononsolvency effect of polymers can be used as a novel trigger<sup>52</sup> to change the size of nanopores in analogy to the opening and closure of the gates of cell membrane channels. We note that achieving any optimization of the concept for some applications requires a quantitative understanding and characterization of the cononsolvency response of nanopore brushes which is the main subject of our work.

Another contribution of our study is that using the suction model for the pressure-driven translocation of the DNA chains and on the basis of the DNA translocation efficiency, for the first time, we were able to quantitatively measure effective hydrodynamic thickness of a polymer layer which is grafted around the rim of nanopores. We envisage that our study will spawn further developments for the design of switchable nanogates and nanopores which are also based on other stimulus-responsive effects such as thermal and pH responses.

## ASSOCIATED CONTENT

### Supporting Information

The Supporting Information is available free of charge at <https://pubs.acs.org/doi/10.1021/acs.macromol.1c00215>.

Details of methods used in this study: method of preparing PNiPAAM-grafted gold membranes; method of identification and counting of DNA translocation

events and the Python source code to realize this method, method of processing data, and information of how to deal with Video Supporting Information; how to estimate grafting density and morphological regime of polymer brushes; additional results of DNA translocation experiments for nanopores; and additional results of the switch effect of PNiPAAM polymer layers on the flat surface both in the ethanol/water mixture and in the ethanol/tris buffer mixtures (PDF)

Identification and counting of DNA translocation events (ZIP)

Python source code to realize the method of processing data (ZIP)

## AUTHOR INFORMATION

### Corresponding Authors

**Huaisong Yong** – Leibniz-Institut für Polymerforschung Dresden e.V., Dresden 01069, Germany; Faculty of Chemistry and Food Chemistry, Technische Universität Dresden, Dresden 01069, Germany; [orcid.org/0000-0003-2317-1585](https://orcid.org/0000-0003-2317-1585); Email: [yong@ipfdd.de](mailto:yong@ipfdd.de)

**Fabien Montel** – Université de Lyon, École Normale Supérieure de Lyon, Université Claude Bernard, CNRS, Laboratoire de Physique, Lyon F-69342, France; Email: [fabien.montel@ens-lyon.fr](mailto:fabien.montel@ens-lyon.fr)

**Jens-Uwe Sommer** – Leibniz-Institut für Polymerforschung Dresden e.V., Dresden 01069, Germany; Institute for Theoretical Physics, Technische Universität Dresden, Dresden 01069, Germany; [orcid.org/0000-0001-8239-3570](https://orcid.org/0000-0001-8239-3570); Email: [sommer@ipfdd.de](mailto:sommer@ipfdd.de)

### Authors

**Bastien Molcrette** – Université de Lyon, École Normale Supérieure de Lyon, Université Claude Bernard, CNRS, Laboratoire de Physique, Lyon F-69342, France

**Marcel Sperling** – Fraunhofer-Institut für Angewandte Polymerforschung, Potsdam-Golm 14476, Germany

Complete contact information is available at: <https://pubs.acs.org/10.1021/acs.macromol.1c00215>

### Author Contributions

H.Y. prepared the manuscript draft. H.Y. and B.M. conducted the experiments. M.S. and H.Y. developed the source code to analyze data of DNA translocation experiments. F.M. and J.-U.S. directed this work. The manuscript was written through contributions of all authors.

### Notes

The authors declare no competing financial interest.

## ACKNOWLEDGMENTS

This work was supported by the Deutsche Forschungsgemeinschaft (DFG) under Grant no. SO 277/17. The authors thank Yixuan Du for experiments of scanning electron microscopy, and the authors thank Holger Merlitz and Jingguo Li for critical reading of the manuscript. The authors also thank Andreas Fery for valuable discussions.

## REFERENCES

- (1) Theato, P.; Sumerlin, B. S.; O'Reilly, R. K.; Epps, T. H., III; Epps, I. Stimuli responsive materials. *Chem. Soc. Rev.* **2013**, *42*, 7055–7056.

- (2) Saha, S.; Weber, C. A.; Nusch, M.; Adame-Arana, O.; Hoegge, C.; Hein, M. Y.; Osborne-Nishimura, E.; Mahamid, J.; Jahnel, M.; Jawerth, L.; Pozniakovski, A.; Eckmann, C. R.; Jülicher, F.; Hyman, A. A. Polar Positioning of Phase-Separated Liquid Compartments in Cells Regulated by an mRNA Competition Mechanism. *Cell* **2016**, *166*, 1572–1584.
- (3) Berry, J.; Brangwynne, C. P.; Haataja, M. Physical principles of intracellular organization via active and passive phase transitions. *Rep. Prog. Phys.* **2018**, *81*, 046601.
- (4) Matsarskaia, O.; Roosen-Runge, F.; Schreiber, F. Multivalent ions and biomolecules: Attempting a comprehensive perspective. *Chemphyschem* **2020**, *21*, 1742–1767.
- (5) Zhang, G.; Wu, C. The Water/Methanol Complexation Induced Reentrant Coil-to-Globule-to-Coil Transition of Individual Homopolymer Chains in Extremely Dilute Solution. *J. Am. Chem. Soc.* **2001**, *123*, 1376–1380.
- (6) Schild, H. G.; Muthukumar, M.; Tirrell, D. A. Cononsolvency in mixed aqueous solutions of poly (N-isopropylacrylamide). *Macromolecules* **1991**, *24*, 948–952.
- (7) Sommer, J.-U. Adsorption–Attraction Model for Co-Non-solvency in Polymer Brushes. *Macromolecules* **2017**, *50*, 2219–2228.
- (8) Yong, H.; Bittrich, E.; Uhlmann, P.; Fery, A.; Sommer, J.-U. Co-Nonsolvency Transition of Poly(N-isopropylacrylamide) Brushes in a Series of Binary Mixtures. *Macromolecules* **2019**, *52*, 6285–6293.
- (9) Coalson, R. D.; Eskandari Nasrabad, A.; Jasnow, D.; Zilman, A. A Polymer-Brush-Based Nanovalue Controlled by Nanoparticle Additives: Design Principles. *J. Phys. Chem. B* **2015**, *119*, 11858–11866.
- (10) Nasrabad, A. E.; Jasnow, D.; Zilman, A.; Coalson, R. D. Precise control of polymer coated nanopores by nanoparticle additives: Insights from computational modeling. *J. Chem. Phys.* **2016**, *145*, 064901.
- (11) Li, C.-W.; Merlitz, H.; Wu, C.-X.; Sommer, J.-U. Nanopores as Switchable Gates for Nanoparticles: A Molecular Dynamics Study. *Macromolecules* **2018**, *51*, 6238–6247.
- (12) Pérez-Mitta, G.; Toimil-Molares, M. E.; Trautmann, C.; Marmisollé, W. A.; Azzaroni, O. Molecular Design of Solid-State Nanopores: Fundamental Concepts and Applications. *Adv. Mater.* **2019**, *31*, No. e1901483.
- (13) Brilmayer, R.; Förster, C.; Zhao, L.; Andrieu-Brunsen, A. Recent trends in nanopore polymer functionalization. *Curr. Opin. Biotechnol.* **2020**, *63*, 200–209.
- (14) Ma, T.; Janot, J. M.; Balme, S. Track-Etched Nanopore/Membrane: From Fundamental to Applications. *Small Methods* **2020**, *4*, 2000366.
- (15) Perez Sirkin, Y. A.; Tagliazucchi, M.; Szleifer, I. Transport in nanopores and nanochannels: some fundamental challenges and nature-inspired solutions. *Mater. Today Adv.* **2020**, *5*, 100047.
- (16) de Groot, G. W.; Santonicola, M. G.; Sugihara, K.; Zambelli, T.; Reimhult, E.; Vörös, J.; Vancso, G. J. Switching transport through nanopores with pH-responsive polymer brushes for controlled ion permeability. *ACS Appl. Mater. Interfaces* **2013**, *5*, 1400–1407.
- (17) Emilsson, G.; Sakiyama, Y.; Malekian, B.; Xiong, K.; Adali-Kaya, Z.; Lim, R. Y. H.; Dahlin, A. B. Gating Protein Transport in Solid State Nanopores by Single Molecule Recognition. *ACS Cent. Sci.* **2018**, *4*, 1007–1014.
- (18) Emilsson, G.; Xiong, K.; Sakiyama, Y.; Malekian, B.; Ahlberg Gagnér, V.; Schoch, R. L.; Lim, R. Y. H.; Dahlin, A. B. Polymer brushes in solid-state nanopores form an impenetrable entropic barrier for proteins. *Nanoscale* **2018**, *10*, 4663–4669.
- (19) Shen, B.; Piskunen, P.; Nummelin, S.; Liu, Q.; Kostianen, M. A.; Linko, V. Advanced DNA Nanopore Technologies. *ACS Appl. Bio Mater.* **2020**, *3*, 5606–5619.
- (20) Zhu, Z.; Wang, D.; Tian, Y.; Jiang, L. Ion/Molecule Transportation in Nanopores and Nanochannels: From Critical Principles to Diverse Functions. *J. Am. Chem. Soc.* **2019**, *141*, 8658–8669.
- (21) Ying, Y.-L.; Long, Y.-T. Nanopore-Based Single-Biomolecule Interfaces: From Information to Knowledge. *J. Am. Chem. Soc.* **2019**, *141*, 15720–15729.
- (22) Lu, S.-M.; Peng, Y.-Y.; Ying, Y.-L.; Long, Y.-T. Electrochemical Sensing at a Confined Space. *Anal. Chem.* **2020**, *92*, S621–S644.
- (23) Hu, Z. L.; Huo, M. Z.; Ying, Y. L.; Long, Y. T. Biological Nanopore Approach for Single-Molecule Protein Sequencing. *Angew. Chem., Int. Ed.* **2021**, *133*, 2–14.
- (24) Cressiot, B.; Bacri, L.; Pelta, J. The Promise of Nanopore Technology: Advances in the Discrimination of Protein Sequences and Chemical Modifications. *Small Methods* **2020**, *4*, 2000090.
- (25) Asandei, A.; Di Muccio, G.; Schiopu, I.; Mereuta, L.; Dragomir, I. S.; Chinappi, M.; Luchian, T. Nanopore-Based Protein Sequencing Using Biopores: Current Achievements and Open Challenges. *Small Methods* **2020**, *4*, 1900595.
- (26) Shi, W.; Friedman, A. K.; Baker, L. A. Nanopore Sensing. *Anal. Chem.* **2017**, *89*, 157–188.
- (27) Howorka, S.; Siwy, Z. Nanopore analytics: sensing of single molecules. *Chem. Soc. Rev.* **2009**, *38*, 2360–2384.
- (28) Auger, T.; Mathé, J.; Viasnoff, V.; Charron, G.; Di Meglio, J.-M.; Auvray, L.; Montel, F. Zero-mode waveguide detection of flow-driven DNA translocation through nanopores. *Phys. Rev. Lett.* **2014**, *113*, 028302.
- (29) Brochard, F.; de Gennes, P. G. Dynamics of confined polymer chains. *J. Chem. Phys.* **1977**, *67*, 52–56.
- (30) de Gennes, P.-G. *Scaling Concepts in Polymer Physics*; Cornell University Press: Ithaca, NY, USA, 1979.
- (31) Zheng, T.; Zhu, M.; Yang, J.; He, J.; Waqas, M.; Li, L. Revisiting the Flow-Driven Translocation of Flexible Linear Chains through Cylindrical Nanopores: Is the Critical Flow Rate Really Independent of the Chain Length? *Macromolecules* **2018**, *51*, 9333–9343.
- (32) Rowghanian, P.; Grosberg, A. Y. Electrophoretic capture of a DNA chain into a nanopore. *Phys. Rev. E: Stat., Nonlinear, Soft Matter Phys.* **2013**, *87*, 042722.
- (33) Grosberg, A. Y.; Khokhlov, A. R. *Statistical Physics of Macromolecules*; American Institute of Physics: New York, USA, 1994.
- (34) Hänggi, P.; Talkner, P.; Borkovec, M. Reaction-rate theory: fifty years after Kramers. *Rev. Mod. Phys.* **1990**, *62*, 251–341.
- (35) Kramers, H. A. Brownian motion in a field of force and the diffusion model of chemical reactions. *Physica* **1940**, *7*, 284–304.
- (36) Huber, P. Soft matter in hard confinement: phase transition thermodynamics, structure, texture, diffusion and flow in nanoporous media. *J. Phys.: Condens. Matter* **2015**, *27*, 103102.
- (37) Bucci, G.; Spakowitz, A. J. Systematic Approach toward Accurate and Efficient DNA Sequencing via Nanoconfinement. *ACS Macro Lett.* **2020**, *9*, 1184–1191.
- (38) Auger, T.; Bourhis, E.; Donnez, J.; Durnez, A.; Di Meglio, J. M.; Auvray, L.; Montel, F.; Yates, J.; Gierak, J. Zero-mode waveguide detection of DNA translocation through FIB-organised arrays of engineered nanopores. *Microelectron. Eng.* **2018**, *187–188*, 90–94.
- (39) Bell, N. A. W.; Muthukumar, M.; Keyser, U. F. Translocation frequency of double-stranded DNA through a solid-state nanopore. *Phys. Rev. E* **2016**, *93*, 022401.
- (40) Wanunu, M.; Morrison, W.; Rabin, Y.; Grosberg, A. Y.; Meller, A. Electrostatic focusing of unlabelled DNA into nanoscale pores using a salt gradient. *Nat. Nanotechnol.* **2010**, *5*, 160–165.
- (41) Chen, Q.; Liu, J.; Schibel, A. E. P.; White, H. S.; Wu, C. Translocation Dynamics of Poly(styrenesulfonic acid) through an  $\alpha$ -Hemolysin Protein Nanopore. *Macromolecules* **2010**, *43*, 10594–10599.
- (42) Oukhaled, A. G.; Biance, A.-L.; Pelta, J.; Auvray, L.; Bacri, L. Transport of long neutral polymers in the semidilute regime through a protein nanopore. *Phys. Rev. Lett.* **2012**, *108*, 088104.
- (43) Yong, H.; Merlitz, H.; Fery, A.; Sommer, J.-U. Polymer Brushes and Gels in Competing Solvents: The Role of Different Interactions and Quantitative Predictions for Poly(N-isopropylacrylamide) in Alcohol–Water Mixtures. *Macromolecules* **2020**, *53*, 2323–2335.

- (44) Gao, K.; Kearney, L. T.; Howarter, J. A. Planar Phase Separation of Weak Polyelectrolyte Brushes in Poor Solvent. *J. Polym. Sci., Part B: Polym. Phys.* **2017**, *55*, 370–377.
- (45) Park, G.; Jung, Y. Many-chain effects on the co-nonsolvency of polymer brushes in a good solvent mixture. *Soft Matter* **2019**, *15*, 7968–7980.
- (46) Jentzsch, C.; Sommer, J.-U. Polymer brushes in explicit poor solvents studied using a new variant of the bond fluctuation model. *J. Chem. Phys.* **2014**, *141*, 104908.
- (47) Choi, B.-C.; Choi, S.; Leckband, D. E. Poly(N-isopropyl acrylamide) brush topography: dependence on grafting conditions and temperature. *Langmuir* **2013**, *29*, 5841–5850.
- (48) Yong, H.; Rauch, S.; Eichhorn, K.-J.; Uhlmann, P.; Fery, A.; Sommer, J.-U. Cononsolvency Transition of Polymer Brushes: A Combined Experimental and Theoretical Study. *Materials* **2018**, *11*, 991.
- (49) Sommer, J.-U. Gluonic and Regulatory Solvents: A Paradigm for Tunable Phase Segregation in Polymers. *Macromolecules* **2018**, *51*, 3066–3074.
- (50) Mills, C. E.; Ding, E.; Olsen, B. D. Cononsolvency of Elastin-like Polypeptides in Water/Alcohol Solutions. *Biomacromolecules* **2019**, *20*, 2167–2173.
- (51) Gilbert, R. J. C.; Serra, M. D.; Froelich, C. J.; Wallace, M. L.; Anderluh, G. Membrane pore formation at protein-lipid interfaces. *Trends Biochem. Sci.* **2014**, *39*, 510–516.
- (52) Binder, W. H. Polymer-induced transient pores in lipid membranes. *Angew. Chem., Int. Ed.* **2008**, *47*, 3092–3095.